



Contents lists available at ScienceDirect

Journal of Cystic Fibrosis

journal homepage: www.elsevier.com/locate/jcf

Original Article

Widespread alterations in systemic immune profile are linked to lung function heterogeneity and airway microbes in cystic fibrosis

Elio Rossi^{a,b,1,*}, Mads Lausen^{a,1}, Nina Friesgaard Øbro^{c,1}, Antonella Colque^a, Bibi Uhre Nielsen^d, Rikke Møller^d, Camilla de Gier^a, Annemette Hald^d, Marianne Skov^e, Tacjana Pressler^{d,e}, Søren Molin^f, Sisse Rye Ostrowski^{c,g}, Hanne Vibeke Marquart^{c,g}, Helle Krogh Johansen^{a,g}

^a Department of Clinical Microbiology, Rigshospitalet, Copenhagen Ø, Denmark

^b Department of Biosciences, University of Milan, Milan, Italy

^c Department of Clinical Immunology, Rigshospitalet, Copenhagen Ø, Denmark

^d Department of Infectious Diseases, Rigshospitalet, Cystic Fibrosis Centre, Copenhagen Ø, Denmark

^e Department of Pediatrics, Rigshospitalet, Cystic Fibrosis Centre, Copenhagen, Denmark

^f Novo Nordisk Foundation Center for Biosustainability, Technical University of Denmark, Kgs. Lyngby, Denmark

^g Department of Clinical Medicine, Faculty of Health and Medical Sciences, University of Copenhagen, Copenhagen N, Denmark

ARTICLE INFO

Keywords:

Cystic fibrosis
Innate immunity
Adaptive immunity
Immune dysregulation
Infections
Lung microbiome

ABSTRACT

Background: Excessive inflammation and recurrent airway infections characterize people with cystic fibrosis (pwCF), a disease with highly heterogeneous clinical outcomes. How the overall immune response is affected in pwCF, its relationships with the lung microbiome, and the source of clinical heterogeneity have not been fully elucidated.

Methods: Peripheral blood and sputum samples were collected from 28 pwCF and an age-matched control group. Systemic immune cell subsets and surface markers were quantified using multiparameter flow cytometry. Lung microbiome composition was reconstructed using metatranscriptomics on sputum samples, and microbial taxa were correlated to circulating immune cells and surface markers expression.

Results: In pwCF, we found a specific systemic immune profile characterized by widespread hyperactivation and altered frequencies of several subsets. These included substantial changes in B-cell subsets, enrichment of CD35⁺/CD49d⁺ neutrophils, and reduction in dendritic cells. Activation markers and checkpoint molecule expression levels differed from healthy subjects. CTLA-4 expression was increased in Tregs and, together with impaired B-cell subsets, correlated with patients' lung function. Concentrations and frequencies of key immune cells and marker expression correlated with the relative abundance of commensal and pathogenic bacteria in the lungs.

Conclusion: The CF-specific immune signature, involving hyperactivation, immune dysregulation with alteration in Treg homeostasis, and impaired B-cell function, is a potential source of lung function heterogeneity. The activity of specific microbes contributes to disrupting the balance of the immune response. Our data provide a unique foundation for identifying novel markers and immunomodulatory targets to develop the future of cystic fibrosis treatment and management.

1. Introduction

Cystic fibrosis (CF) is a monogenic disease caused by mutations in the *CFTR* gene and is one of the most common autosomal recessive genetic

disorders. *CFTR* encodes a chloride channel highly expressed in epithelial cells in various tissues, making CF a multi-organ disease.

CF lung disease is complex and has diverse clinical outcomes [1]. It is characterized by an early onset of chronic inflammation and recurrent

* Corresponding author: Elio Rossi, Via Celoria 26, 20133, Milan, Italy.

E-mail address: elio.rossi@unimi.it (E. Rossi).

¹ Equal contribution

<https://doi.org/10.1016/j.jcf.2024.04.015>

Received 18 February 2024; Received in revised form 23 April 2024; Accepted 26 April 2024

1569-1993/© 2024 The Authors. Published by Elsevier B.V. on behalf of European Cystic Fibrosis Society. This is an open access article under the CC BY-NC-ND license (<http://creativecommons.org/licenses/by-nc-nd/4.0/>).

bacterial airway infections, the primary cause of morbidity and mortality. Ongoing pulmonary inflammation and infections lead to structural lung damage and a progressive loss of lung function. It remains unclear whether persistent infections primarily trigger an aberrant inflammatory response or whether it is a precondition that favors microbial colonization. In CF, the immune system fails to resolve the inflammatory response and provide protective immunity against pulmonary infections, showing that the CF immune system is highly dysfunctional [2]. Thus, flaws in the immune response are directly linked to disease severity in CF.

It is critical to understand whether the CF immune system is dysregulated and what mechanisms drive these defects. Innate and adaptive immune cell populations are functionally affected in CF [3], and these deficiencies have been directly linked to *CFTR* mutations rather than active infections [4]. However, the *CFTR* genotype alone cannot explain the heterogeneous disease phenotypes observed in people with CF (pwCF). Therefore, several other factors, such as mutations in modifier genes, sex, metabolic differences, and the lung microbiota, have been suggested to contribute to the disease phenotype [5]. For example, increased lung microbiome diversity in pwCF correlates positively with lung function [6]. In vitro, commensal bacteria isolated from CF airways can reduce the inflammation induced by the common CF pathogen *Pseudomonas aeruginosa* [7]. Thus, the CF lung microbiome is likely a significant contributing factor modulating the CF immune system, but this remains to be demonstrated.

In this work, using high-resolution flow cytometry and metatranscriptomics analysis on blood and sputum samples, respectively, we investigate the composition and activation status of all immune cell compartments and the transcriptionally active lung microbial communities. Overall, we reconstruct a detailed picture of the immune profile that differentiates CF patients from healthy individuals, identifying alterations in Tregs homeostasis and B-cell responses as a possible source of the clinical heterogeneity observed in the patient's lung function. Finally, we provide evidence of specific associations between beneficial and pathogenic microbes with a subset of circulating immune cells.

2. Results

2.1. Demographics of the study cohort

Twenty-eight pwCF attending the Copenhagen CF center at Rigshospitalet were consecutively recruited (Table 1). The cohort was predominantly males (61%) with a median age of 34 years (range 12 - 61). Most pwCF were characterized by homozygous *CFTR* $\Delta F508$ mutation (67.9%), while only 28.6% had a secondary mutation in addition to $\Delta F508$. All mutations were classified as severe. Almost all patients were clinically defined as chronically infected by *Pseudomonas aeruginosa* (89.3%, Copenhagen criteria [8]) and had a median percent predicted forced expiratory volume in 1 s (ppFEV₁) of 62% ranging between 24 - 99%. Except for one, all pwCF were diagnosed with pancreatic insufficiency. Only eight pwCF (28.6%) were not treated with CFTR modulators, while the rest were on Ivacaftor/tezacaftor (35.7%), Ivacaftor/tezacaftor/eleacaftor (17.9%), Ivacaftor/lumacaftor (14.3%) or Ivacaftor (3.6%) (Table 1, Supplementary Data 1).

Most pwCF were treated with oral azithromycin alone (57.1%) or in combination with ciprofloxacin (14.3%). Few were treated with ciprofloxacin (10.7%) alone or in combination with amoxicillin and clavulanic acid (3.4%) (Table 1, Supplementary Data 1). In most cases, oral antibiotics were combined with inhalation of aztreonam (28.6%), colistin (25.0%), or tobramycin (10.7%) alone or in combination with colistin (7.1%), or ceftazidime (3.6%) or piperacillin+tazobactam together with voriconazole (Table 1 and Supplementary Data 1). Three pwCF were not compliant and did not take any prescriptions for six months before enrollment. In addition, 27 age- and sex-matched healthy subjects were included anonymously from the Blood Bank, Department of Clinical Immunology at Rigshospitalet (Table 1).

Table 1
Study cohort demographics and treatments.

Demographics	CF cohort	Control cohort	P value	Test
All (%)	28 (100)	27 (100)		
Sex				
Female, n (%)	11 (39.3)	15 (55.6)	0.285	Fisher's exact
Male, n (%)	17 (60.7)	12 (44.4)		
Age, median (range)	34 (12 - 61)	36 (24 - 65)	0.167	Mann-Whitney
FEV ₁ %, median (range)	62 (24 - 99)	..		
Pancreatic insufficiency				
Yes, n (%)	27 (96.4)	..		
No, n (%)	1 (3.6)	..		
Mutation				
F508 homo, n (%)	19 (67.9)	..		
F508 hetero, n (%)	8 (28.6)	..		
Other, n (%)	1 (3.6)	..		
Chronic <i>P. aeruginosa</i> , n (%)	25 (89.3)	..		
Treatments				
CFTR modulator				
Ivacaftor/tezacaftor/eleacaftor, n (%)	5 (17.9)	..		
Ivacaftor, n (%)	1 (3.6)	..		
Ivacaftor/lumacaftor, n (%)	4 (14.3)	..		
Ivacaftor/tezacaftor, n (%)	10 (35.7)	..		
Nothing, n (%)	8 (28.6)	..		
Antibiotics (<i>per oral</i>)				
Azithromycin, n (%)	16 (57.1)	..		
Azithromycin/ciprofloxacin, n (%)	4 (14.3)	..		
Ciprofloxacin, n (%)	3 (10.7)	..		
Ciprofloxacin/Amoxicillin+Clavulanic Acid, n (%)	1 (3.6)	..		
Nothing, n (%)	4 (14.3)	..		
Antibiotics (inhaled)				
Aztreonam, n (%)	8 (28.6)	..		
Ceftazidime, n (%)	1 (3.6)	..		
Colistin, n (%)	7 (25.0)	..		
Piperacillin+Tazobactam/voriconazole, n (%)	1 (3.6)	..		
Tobramycin, n (%)	3 (10.7)	..		
Tobramycin/colistin, n (%)	2 (7.1)	..		
Nothing, n (%)	6 (21.4)	..		

2.2. Multiple immunological compartments contribute to defining the CF systemic immune profile

To gain insight into the CF immunophenotype, we made a comprehensive whole-blood analysis of immune cell composition and their activation states in pwCF and healthy subjects. Principal component analysis of the absolute concentration (cells/ml) of 82 immune cell subtypes indicated that pwCF clustered separately from healthy subjects (Fig. 1A). Diverse branches of innate and adaptive immunity contributed to the CF immune profile (Fig. 1A). In pwCF, neutrophil concentration was almost twice as high, while dendritic cells (DCs) and CD4⁺ T cell

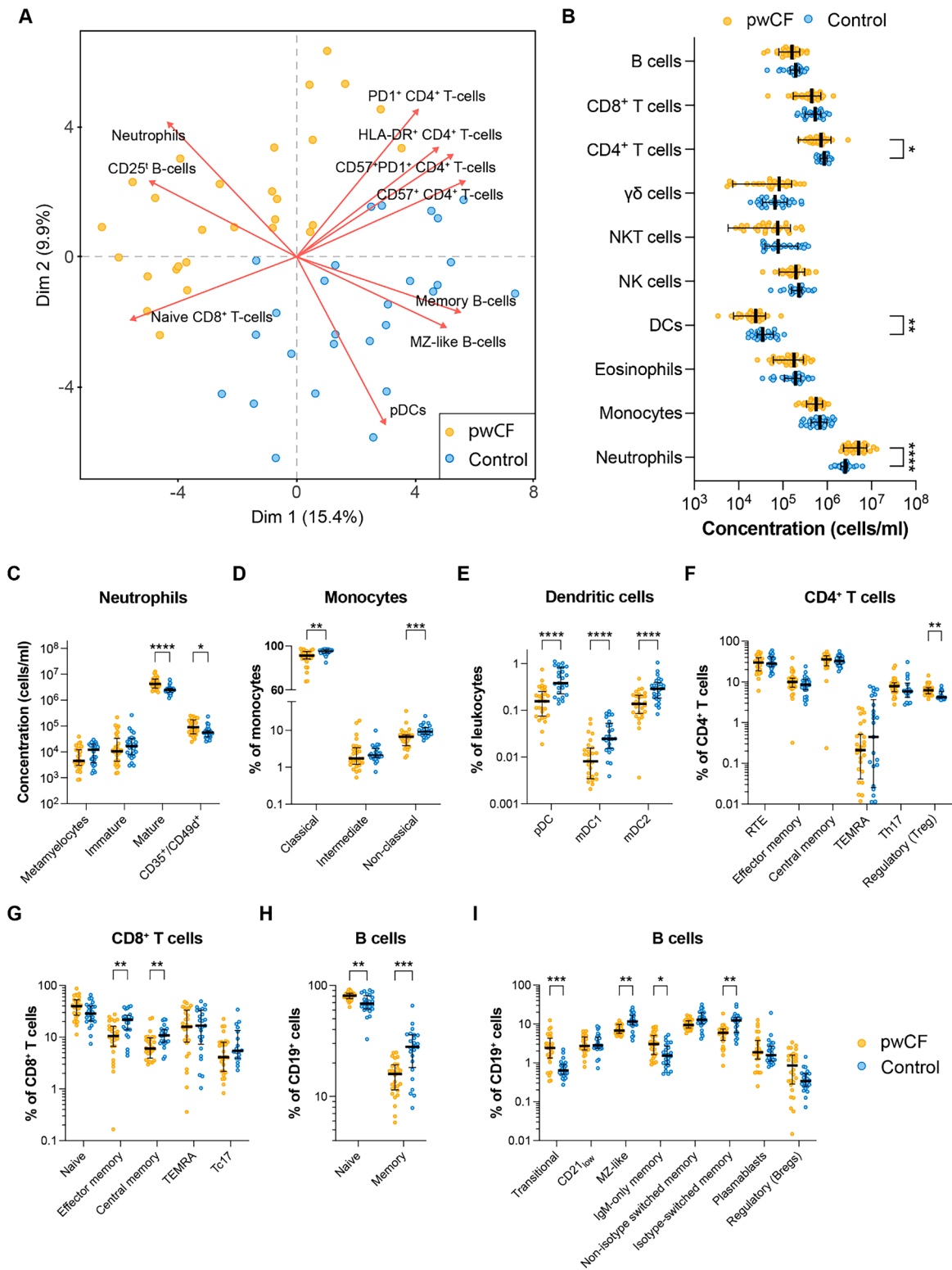


Fig. 1. Circulating immune cells characterizing people with cystic fibrosis (pwCF). **A.** Principal component analysis (PCA) of cell frequencies in whole blood from pwCF and sex- and age-matched healthy subjects (control). The first two principal components (Dim) are plotted. Points represent individual subjects' data color-coded by subject type (orange: pwCF; blue: control). Loadings of the top 10 contributing variables to Dim1 and Dim2 are shown. **B.** Dot plots represent the median concentration of the major immune cell types (cells/ml). Dots represent the concentration in individual subjects (orange: pwCF; blue: control). Two-sided Wilcoxon test with Benjamini & Hochberg multiple testing correction: *, adjusted P value ≤ 0.05 ; **, adjusted P value ≤ 0.01 ; ****, adjusted P value ≤ 0.0001 . **C - J.** Dot plots represent the median concentration of specific cell types (cells/ml) or the frequency of parent populations (% of parent cells). Dots represent the value of individual subjects (orange: pwCF; blue: control). Two-sided Wilcoxon test with Benjamini & Hochberg multiple testing correction: *, adjusted P value ≤ 0.05 ; **, adjusted P value ≤ 0.01 ; ***, adjusted P value ≤ 0.001 ; ****, adjusted P value ≤ 0.0001 .

concentrations were 1.8- and 1.2-fold lower (Fig. 1B). All other major immune cell classes showed tendencies towards being reduced in pwCF, although not statistically significant.

Analysis of the myeloid subpopulations showed that the high neutrophil concentration in pwCF was due to increased concentrations of mature CD10⁺ neutrophils and neutrophils with co-expression of CD35⁺/CD49d⁺ (Fig. 1C). We observed an overall reduction of non-classical (CD14^{low}CD16^{hi}) and classical circulating monocytes (CD14^{hi}CD16^{low}) in pwCF (Fig. 1D). Plasmacytoid dendritic cells (pDC) and CD1c⁺CD141⁻ (mDC1) and CD1c⁻CD141⁺ (mDC2) myeloid dendritic cells were reduced in pwCF (Fig. 1E).

Concerning the acquired cell-mediated immunity, we observed a reduction in CD4⁺ T-cell concentration in pwCF (Fig. 1B), with a normal distribution of CD4⁺ T-cell subsets except for an increased fraction of

FOXP3⁺ regulatory T cells (Tregs) (Fig. 1F). In contrast, CD8⁺ T-cell subpopulations were altered with a decrease in the absolute concentration and fraction of CD8⁺ effector memory T cells, CD8⁺ central memory T cells, and CD161⁺CD196⁺CD8⁺ T cells (Tc17 cells) (Fig. 1G and Fig. S1A).

Finally, the total B-cell concentration in pwCF was within the normal range of healthy subjects (Fig. 1B). Still, pwCF were characterized by a substantially higher fraction of naïve (CD27⁻) B cells paralleled by a reduction in the memory (CD27⁺) B cells (Fig. 1H). Further, pwCF had higher fractions of transitional (IgM⁺CD38⁺CD27⁻) B cells (Fig. 1I), the early, immature B-cell stage, recently emigrated from the bone marrow. In contrast, the fraction of CD27⁺ marginal zone-like (MZ-like) B cells and isotype-switched memory B cells were reduced in pwCF. In contrast, the IgM⁺IgD⁻ memory B-cell subset (IgM-only memory B cells) was

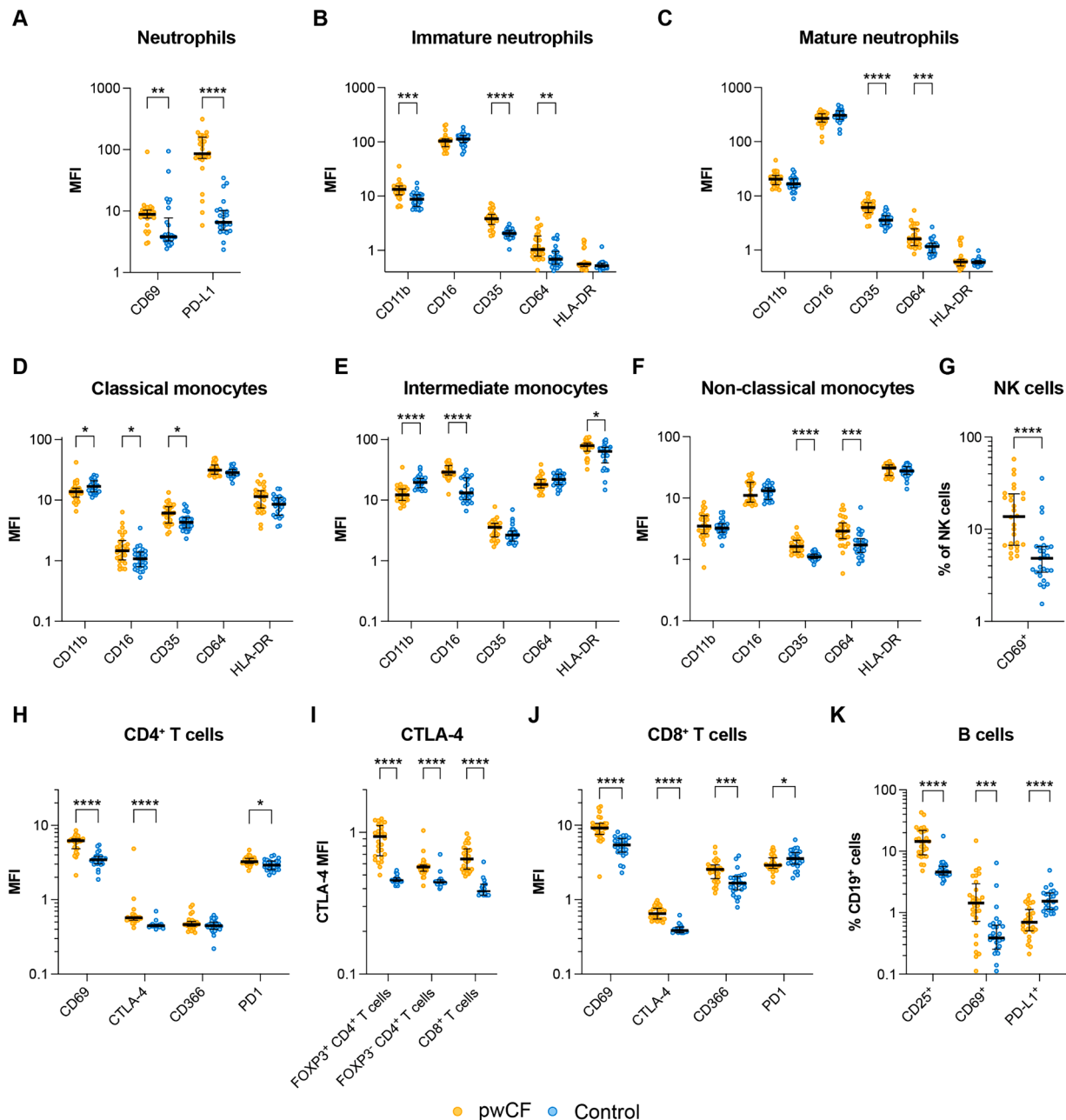


Fig. 2. Activation and regulation of immune cells in people with cystic fibrosis (pwCF) and healthy subjects (control). A – K. Dot plots represent cell activation or regulatory surface markers' median fluorescence intensity (MFI) or the median fraction of parent populations (% of parent cells). Dots represent individual subjects (orange: pwCF; blue: control). Two-sided Wilcoxon test with Benjamini & Hochberg multiple testing correction: *, adjusted *P* value ≤ 0.05; **, adjusted *P* value ≤ 0.01; ***, adjusted *P* value ≤ 0.001; ****, adjusted *P* value ≤ 0.0001.

elevated (Fig. 1I).

2.3. Expression of activation markers and check-point molecules indicates hyperactivated immune cells and immune dysregulation

The *CFTR* mutation is associated with dysfunction of immune cell function and activation [9]. Therefore, we investigated the expression of surface markers involved in the regulation and activation of immune cells.

Several activation markers were upregulated on CF neutrophils. The lectin CD69 (Fig. 2A), the complement receptor 1 (CD35), and the Fc receptor CD64 were increased approximately 1.5 times on immature and mature neutrophils (Fig. 2B and 2C). CD11b, an integrin involved in phagocytosis and adhesion, was more abundantly expressed (1.5-fold) on immature CF neutrophils (Fig. 2B). The checkpoint molecule Cell Death Protein-Ligand 1 (PD-L1) on PD-L1⁺ neutrophils was 13 times higher in pwCF (MFI: 85.7 vs. 6.6, $p < 0.0001$) (Fig. 2A) and the fraction of PD-L1⁺ neutrophils was twice as high in (0.17% vs. 0.075%, P value = 0.026) in pwCF than in healthy subjects (Fig. S1B).

Like neutrophils, circulating CF monocytes displayed an activated phenotype with changes in the expression of receptors essential for phagocytosis, migration, and antigen presentation. In pwCF, classical monocytes showed a 1.2-fold decrease in CD11b expression, while CD16 and CD35 receptors expression increased 1.6 and 1.4 times, respectively (Fig. 2D). Intermediate CF monocytes (CD14^{int}CD16^{int}) had decreased CD11b (1.7-fold) and increased expression of CD16 (1.9-fold) and HLA-DR (1.3 fold) (Fig. 2E). In comparison, non-classical monocytes had increased surface expression of CD35 (1.5-fold) and CD64 (1.7-fold) (Fig. 2F). We also observed a 1.4-fold increase of CD366 (TIM-3/T-cell immunoglobulin and mucin-domain containing-3) expression on CF monocytes (Fig. S1C). The exact role of CD366 in monocytes is not fully understood, but CD366 may be a negative regulator of monocyte IL-12 production with the potential to regulate adaptive Th1 response [10].

Dendritic cells showed no difference, except for a decreased expression on mDCs of CD301 (Fig. S2), a C-type lectin important in regulating exaggerated B-cell responses [11] and suppression of autoantibodies.

The NK cell concentration was normal in pwCF; however, the fraction of activated CD69⁺ NK cells in pwCF was almost three times higher than in controls (13.7% vs. 4.8%) (Fig. 2G).

Similarly, CF T cells demonstrated an activated phenotype compared to healthy subjects. Non-regulatory FOXP3⁻ CD4⁺ T cells had increased surface expression of the early activation marker CD69 and the immune checkpoint receptors CTLA-4 (cytotoxic T-lymphocyte associated protein-4) and PD1 (Fig. 2H). Additionally, we observed a 2.4-fold increase in CTLA-4 levels on regulatory FOXP3⁺ CD4⁺ T cells (Tregs) in pwCF (Fig. 2I). Also, CF CD8⁺ T cells showed a difference in surface marker expression with increased expression of CD69 and CTLA-4 together with the checkpoint molecule CD366. However, CD8⁺ T-cell expression of PD1 was reduced in pwCF (Fig. 2J), suggesting that the PD1/PD-L1 axis may be differentially regulated in CD4⁺ and CD8⁺ T cells of pwCF.

Increased immune activation also affected B cells. We observed increased fractions of B cells expressing the CD25 and CD69 activation markers (Fig. 2K), while the B-cell fraction expressing the PD1 ligand (PD-L1) was reduced in pwCF (Fig. 2K). However, the level of PD-L1 expression on the cell surface of PD-L1⁺ B cells was higher in pwCF (Fig. S1D), further highlighting the dysregulation in the B-cell compartment and the PD1/PD-L1 immune checkpoint.

2.4. The CF systemic immune profile is linked to lung function

Although a specific peripheral blood immune cell profile characterized pwCF, the clinical phenotypes are often heterogeneous. Thus, we investigated whether the immune profile variations within the CF cohort were associated with patients' clinical parameters. Average silhouette

and gap statistics indicate that pwCF could be separated into two groups (C1, $n = 15$; C2, $n = 13$) using K-means clustering based on normalized absolute concentration of circulating immune cells (Fig. 3A). Comparing CF disease parameters between the two clusters showed that patients in C1 had significantly better lung function (ppFEV₁) than those in C2 (median ppFEV₁: 73 vs. 41, $P = 0.0054$) (Fig. 3B and Table S4). No significant differences were observed for other clinical and demographic parameters such as BMI, CF-related diabetes, total IgG levels, *CFTR* mutation, years since the first *P. aeruginosa* isolates, sex, age, and potential immunomodulatory treatments such as *CFTR* modulators [12] or azithromycin [13] (Table S3); thus, a specific link between disease severity heterogeneity and the overall abundance of different immune cell types at a systemic level might exist. C1 was characterized by an increase in the absolute concentration of several immune cell populations belonging to innate and adaptive immunity (Fig. 3C). Significant differences were observed in the B-cell subpopulations, including isotype-switched memory B cells, i.e., cells able to quickly produce efficient pathogen-specific antibodies after antigen reactivation, suggesting an overall increase in cells involved in the protective B-cell response in C1 patients.

Then, we further explored the dependence of patients' lung function on the circulating immune cell state, independently correlating the ppFEV₁ parameter with the normalized absolute counts and the cell frequencies of all immune cell types, as well as the expression level of all surface markers. As expected, the absolute concentration of B cells, particularly of naïve, MZ-like, and memory B-cell subpopulations and classical monocytes, showed a significant positive correlation with ppFEV₁ (Fig. 3D). Similarly, a higher fraction of the CD35⁺/CD49d⁺ neutrophils subset and CD4⁺ recent thymic emigrants (CD4⁺ RTE) were positively associated with improved lung function (Fig. 3D). In contrast, the fraction of natural killer T (NKT) cells, mature neutrophils, intermediate monocytes, and elevated levels of CD21^{low} B cells negatively correlated with ppFEV₁. Among all activation/regulation markers tested, only the expression of the immune checkpoint regulator CTLA-4 on Tregs and conventional T helper cells correlated positively with ppFEV₁.

2.5. Systemic immune profiles associate with specific lung microbes but have no direct links with the overall microbiome

Pathogens actively colonizing pwCF airways are known to influence the immune system [14]. Therefore, we explored potential links between the active lung microbial community and the systemic immune system within the pwCF cohort. We collected sputum samples from 26 of the 28 patients and reconstructed the composition of the transcriptionally active microbiome using a metatranscriptomics analysis. The microbiomes recovered were complex. We observed the co-occurrence of several pathogens commonly associated with CF infections, including bacteria from the *Pseudomonas*, *Stenotrophomonas*, *Mycobacterium*, *Hemophilus*, and *Staphylococcus* genera, and fungi from the *Aspergillus* and *Saccharomyces* genera (Fig. S3). *Pseudomonas* could be detected at variable percentages (0.04% - 99.9%) (Fig. S3 and Supplementary Data 2) in all pwCF despite a small fraction of patients being not clinically defined as chronically infected (Table 1). At first, we evaluated whether the two groups of pwCF showing different lung function levels and immune profiles we identified earlier were characterized by specific microbiomes. PERMANOVA analysis on samples' β -diversity indicated that the transcriptionally active microbiomes did not differ between the two groups (PERMANOVA, $P = 0.411$). Thus, the differences in the overall composition of the lung microbiomes have no apparent effect in defining the complete immune profiles observed in peripheral blood. However, microbiome composition was significantly associated with ppFEV₁ (Mantel test, $r = 0.173$; $P = 0.016$), indicating a partial contribution of the microbiome to lung function.

Then, we searched for specific associations between the relative abundance of the most frequent microbial genera (relative abundance of

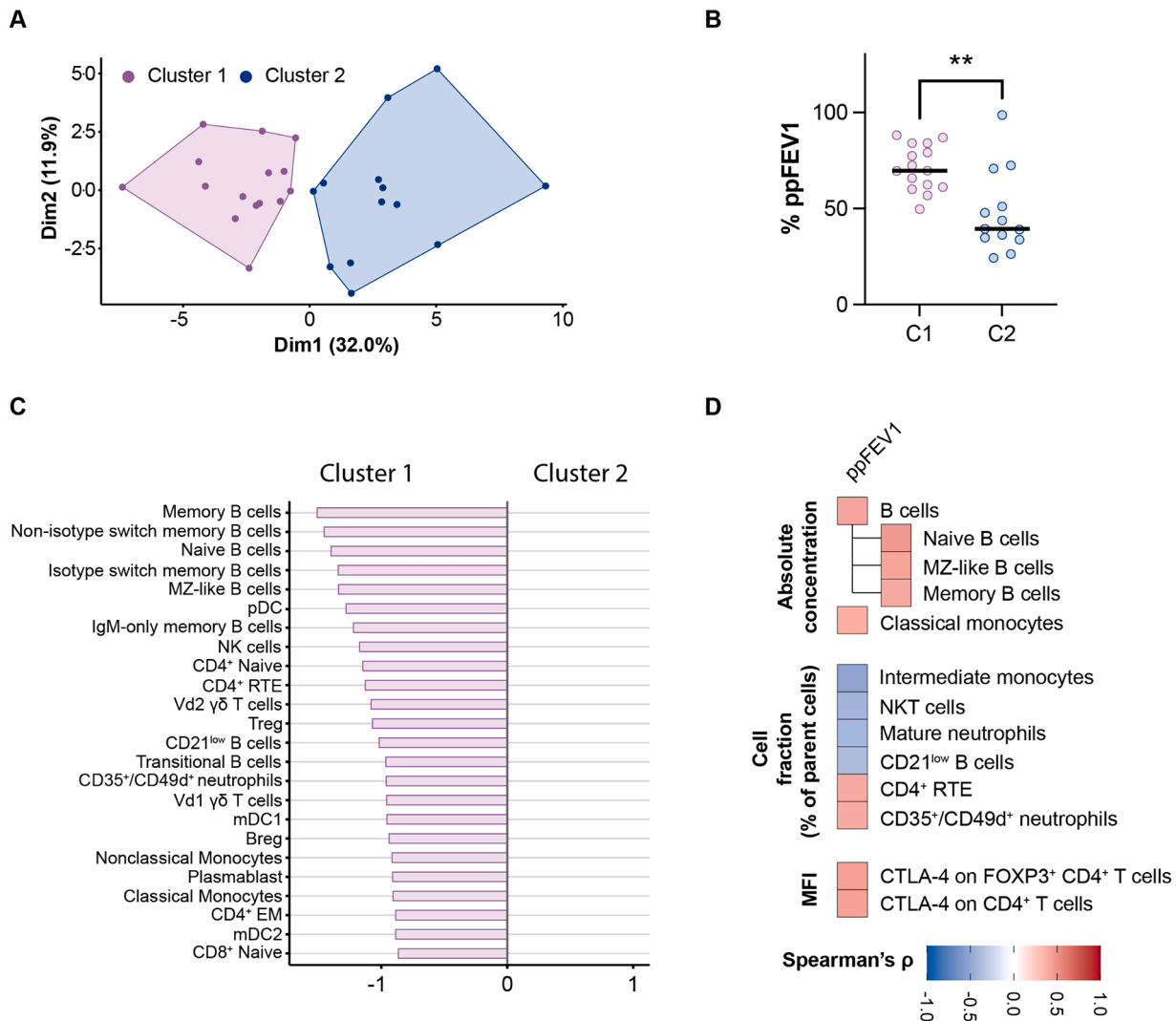


Fig. 3. Immunophenotypic variation within the cystic fibrosis (CF) cohort and its relationship with lung function. A. Clustering of people with CF (pwCF) based on K-means clustering using normalized cell concentrations. The optimal number of clusters was identified using average silhouette and gap statistics. C. Diverging bar chart representing Z-score differences of significantly different cell populations between patient clusters based on Two-sided Wilcoxon test with Benjamini & Hochberg multiple testing correction. D. Correlation heatmaps showing only significant correlations between the lung function predictor ppFEV₁ and immune cell absolute concentrations, immune cell frequencies, and surface markers expression. Spearman's rho rank correlation analysis with $P < 0.05$ was considered statistically significant.

1% in at least one-fifth of the patients) and different immunological variables, including the absolute concentration of immune cells, distribution of cell subsets, and surface expression levels of activation and checkpoint molecules. The relative genera abundance of *Mycobacterium*, *Staphylococcus*, and the commensal *Veillonella* showed the most significant correlations, whereas the *Pseudomonas* genus showed the lowest (Fig. S4). Further, based on all significant correlations identified, pathogenic genera (*Mycobacterium*, *Aspergillus*, *Staphylococcus*) clustered together, except for *Pseudomonas*, which showed correlation patterns more similar to oral commensal genera (*Streptococcus*, *Veillonella*, *Prevotella*, *Rothia*, and *Gemella*) (Fig. 4A-C). Overall, commensal taxa correlated positively with the concentration and fraction of several circulating cells, in particular of those of lymphoid lineage, such as activated CD69⁺ B cells, CD4⁺ and CD8⁺ T-cell subtypes, and regulatory B cells, which were reduced with increasing amounts of the pathogens such as *Staphylococcus*, *Aspergillus*, and *Mycobacterium*. Concentration and fraction of PD-L1⁺ B cells, granulocytes, monocytes, CD69⁺ neutrophils, and Tc17 cells positively correlated with the increasing abundance of pathogens while showing a negative correlation with the abundance of commensal genera (Fig. 4A and 4B), indicating intra-

cohort differences in the PD1/PD-L1 axis.

Similarly, we observed the same tendency with the level of surface markers. Immune activation markers, such as CD69, CD64, CTLA-4, and CD25, and other surface markers, including CD16, CD11b, and CD301, showed an opposite correlation between the abundance of pathogens and commensal bacteria.

2.6. Discussion

In our study, we characterized a distinct immune profile in the peripheral blood of pwCF and its associations with lung function heterogeneity and the airway microbiome, highlighting potential prognostic markers and immune targets in the innate and adaptive immune response. However, our findings are based on a single site and require further replication for broader generalization.

The CF immune profile shared traits common to autoimmune and chronic inflammatory diseases, with widespread immune activation and dysregulation in different immunological compartments. We observed several known CF hallmarks: increased neutrophil [15], reduced CD4⁺ T cells [16], and decreased circulating dendritic cells (DCs) [17]. The

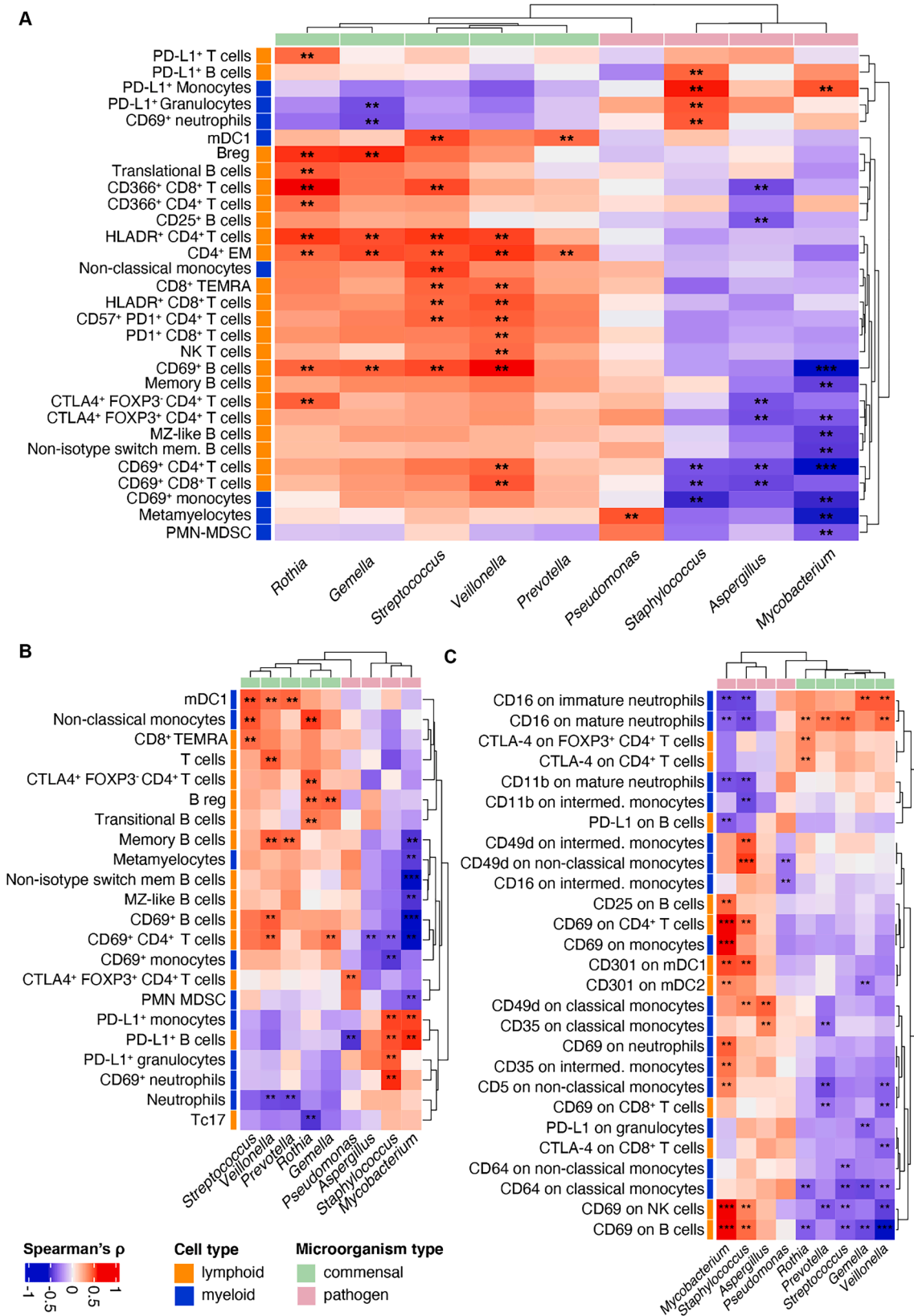


Fig. 4. Association between the systemic immune phenotype and the lung microbiome in people with cystic fibrosis (pwCF). Heatmaps showing all statistically significant correlations (marked with asterisks) between immune cell absolute concentrations (cells/ml, **panel A**), frequencies (% of the parent immune cell type, **panel B**), and median fluorescence intensity (MFI) of cell surface activation markers (**panel C**). Correlations were calculated by Spearman's rho rank correlation analysis with a *P* value < 0.05 considered statistically significant. *, *P* value < 0.05; **, *P* value < 0.01; ***, *P* value < 0.001. Immune cell type derivation (lymphoid or myeloid) and microorganism type (commensal or pathogen) are reported.

increase in circulating neutrophils was not limited to mature neutrophils but depended on a CD35⁺/CD49d⁺-double-positive subpopulation. A proper balance of CD49d⁺ neutrophils is necessary to resolve bacterial infections [18], while high concentrations of this subpopulation relate to defective resolution of inflammation [19] and a predisposition to hypersensitivity reactions [20], a common condition in pwCF [21]. Although potentially exposing to co-morbidities, higher concentrations of CD35⁺/CD49d⁺ co-expressing neutrophils characterized a subgroup of pwCF with better lung function and, overall, higher CD35⁺/CD49d⁺ neutrophil frequency positively correlated with ppFEV₁.

Immune dysregulation, i.e., the breakdown of the molecular control of immune system processes, leads to disturbed selection or activation of immune cells, impaired regulatory T-cell (Tregs) homeostasis, and increased danger signaling in autoimmune and autoinflammatory diseases. The altered microbiome and defects in the epithelial barrier permeability are factors contributing to immune dysregulation [22]. T-cell responses are dysregulated in pwCF, with a marked shift toward a Th2- and Th17-dominated response [23]. This effect depends on quantitative and qualitative impairment of Tregs homeostasis occurring after *P. aeruginosa* infections [16]. Although we observed an overall reduction in CD4⁺ T-cell concentrations, in contrast to previous findings [16], Tregs fraction was higher in pwCF. No apparent correlation between Tregs fraction and ppFEV₁ could be detected, even though *P. aeruginosa* was identified in the airway microbiome of all patients analyzed. However, the pathogen was dominant only in a fraction of patients, and we observed a correlation of CTLA-4⁺ Tregs concentration and fraction with the relative abundance of different microorganisms, increasing with *Pseudomonas* and decreasing with *Aspergillus* and *Mycobacterium*. These discrepancies might stem from the active microbial community at sampling time, suggesting that microorganisms can differentially influence Tregs homeostasis and the balance between adequate pathogen clearance and the development of an uncontrolled inflammatory response [24].

Upregulation of CTLA-4 expression on Tregs cells of pwCF further supported the central role of Tregs in defining CF disease. CTLA-4 is essential for Tregs homeostasis and immuno-suppressive function, thus indicating a specific immune dysregulation that might account for the reduction of a beneficial response and increased pathogen persistence [24].

Nevertheless, our data indicated that CTLA-4 expression level, and thus its regulatory function on Tregs and classic CD4⁺ T cells, positively correlated with patients' ppFEV₁ parameter and, thus, with lung function. CTLA-4 upregulation on the two cell types was linked with the relative abundance of the *Rothia* genus. *Rothia mucilaginosa* can reduce inflammation by modulating the NF- κ B pathway [25], which is also involved in regulating Tregs development and function and might be the source for CTLA-4 changes observed in pwCF.

The CF immune phenotype also showed quantitative and qualitative changes in circulating dendritic cells (DCs). DCs absolute concentration was significantly reduced in pwCF, resembling other respiratory diseases characterized by chronic inflammation and recurrent microbial infections [26]. Further, the C-type lectin CD301 expression on myeloid dendritic cells (mDCs) was lower in pwCF. Levels of CD301 on mDCs might also be modulated in response to active microbes: CD301 expression correlated positively with the relative abundance of the pathogenic taxa *Mycobacterium* and *Staphylococcus*. In contrast, the marker expression reduced with the increasing abundance of commensal taxa, specifically the *Gemella* genus. Depletion of CD301⁺ DCs relates to an impaired Th2 response upon nematode infections [27], and CD301⁺ DCs are necessary for IL-17 production from TCR γ δ T cells and Th17 cells following intranasal infection with *Streptococcus pyogenes* [28]. The overall reduction of CD301 and CD301⁺ DCs might contribute to Th17-skewed production of the proinflammatory cytokine IL-17 and modulation of the Th1 and Th2 responses.

CD301 expression by DCs also plays a role in B-cell maturation and activity. CD301 depletion correlates with the increasing generation of

autoreactive antibodies [11], found in up to 80% of pwCF [29]. Although we could not verify this association in our cohort, we observed significant B-cell compartment dysfunction in pwCF. Despite having absolute B-cell concentrations comparable to healthy subjects, pwCF showed reduced MZ-like and isotype-switched memory B-cell fractions and increased fractions of naïve B cells and IgM-only memory B cells. These characteristics are observed in other chronic lung diseases, such as bronchiectasis [30], as well as in individuals affected by common variable immunodeficiency (CVID), a primary immunodeficiency disease with reduced ability to isotype-switch and recurrent airway infections due to low levels of protective antibodies [31]. pwCF reduced capacity for isotype-switch and development of memory may compromise the high-affinity secondary antibody responses, contributing to recurrent opportunistic infections.

Despite showing a peculiar immune phenotype, clinical outcomes in pwCF are heterogeneous, particularly at the level of lung function. B-cell function might be relevant in defining these differences. We identified a subgroup within the pwCF cohort with better lung function and higher absolute concentrations of several B-cell subtypes. Although B cells were similar between healthy subjects and pwCF when taken as a whole, some pwCF may maintain a better B-cell response in absolute terms. Once recruited from the bloodstream to inducible bronchus-associated lymphoid tissue (iBALT), i.e., ectopic lymphoid tissues present in pwCF due to recurrent infections [32], higher B-cell function might offer better protection against pathogens resulting in a slower decline of lung function. Further, pwCF with higher ppFEV₁ had higher concentrations of regulatory B cells, which might contribute to preventing uncontrolled inflammation via the production of anti-inflammatory mediators, thus containing lung damage [33]. Yet, an increased fraction of CD21^{low} B cells was associated with a worse lung function. The CD21^{low} subset is expanded in conditions characterized by chronic immune stimulation, as in CVID patients where CD21^{low} cells are associated with autoimmune disease [34]. Elevated fractions of CD21^{low} B cells may represent, if not properly balanced, another player in determining diversity in pwCF clinical outcomes, as in CVID patients [35].

Our work cannot clarify whether the differences we observed in pwCF were intrinsic or acquired due to the infection history. The role of the microbiome in CF and inflammation is still debated [14]. Commensal bacteria might reduce hyperinflammation induced by *P. aeruginosa* [7], but enrichment of oral taxa in the lung is associated with a Th17-dependent inflammatory response [36].

Our data suggested that the microbial community can influence the balance of the immune response. Commensal bacteria and opportunistic pathogens showed distinct and opposite correlation profiles for several immunological variables: *Prevotella*, *Rothia*, *Veillonella*, and *Gemella* positively correlated with the abundance and frequency of several lymphoid cells that were also enriched in patients with higher ppFEV₁ levels. Likewise, the abundance of commensals negatively correlated with several activation markers on myeloid and lymphoid cells, with pathogenic taxa showing an opposite trend. We could not prove that the correlations were biologically relevant, and our data was limited to sputum samples, which, although considered a good approximation of the average microbiome in the lungs [37], may not reliably sample all airway niches. Although with limitations, our observations indicated that oral commensals can promote the activity of the overall immune system, avoiding immune hyperactivation connected with the increasing presence of pathogenic taxa, in agreement with previous studies [25,38,39].

Among pathogens, the *Pseudomonas* genus represented an interesting case. We observed a positive correlation between *Pseudomonas* and metamyelocytes. Still, we did not detect any significant correlation with other immunological variables despite the known role of *P. aeruginosa* in CF pathogenesis. This discrepancy highlights an important limitation of our study design and may be attributed to several factors. The bacterium could be detected at variable levels in all pwCF, potentially masking changes in immune variables and limiting our ability to evaluate the

impact of *P. aeruginosa*. Additionally, the effects of this pathogen may be minimal at the systemic level. As we solely investigated circulating immune cells, changes at the site of infection may have gone unnoticed.

Similarly, our approach cannot easily predict the effect of circulating cells on the responses happening at the site of infection and does not account for tissue-resident cells, which are crucial for lung disease after chronic exposure to pathogens [40]. Further, the expression of surface markers and checkpoint molecules does not allow the evaluation of functional impairments of immune cells, such as defective bacterial killing by CF neutrophils and macrophages [15]. Likewise, HLA haplotypes were not considered in the study. However, class II MHC (major histocompatibility complex) is a gene modifier in CF [41] and can influence immune response, infection susceptibility, and lung disease [42]. Finally, our analysis may have overlooked other important cell types defining CF pathology and lung disease.

Despite the efficacy of CFTR modulators in reducing traditional CF pathogens, a significant proportion of patients remain infected [43]. This underscores the need for a more comprehensive understanding of host-pathogen interactions in pwCF. Our work highlights how the overall immune system is affected in pwCF, identifying several traits similar to other patients suffering from immune disorders. It provides a crucial foundation for developing evidence-based medicine and suggests that the coexistence of various members of microbial communities may influence the immune response in CF. Consequently, any immune modulatory intervention should acknowledge the complex interactions with the microbiome occurring during the treatment.

3. Methods

3.1. Samples collection and pre-processing

Peripheral blood samples were collected in three separate tubes (K_2EDTA , 3 ml; Sodium Citrate, 3.5 ml; Lithium Heparin, 4 ml) by venipuncture and processed for flow cytometry staining the same day. At the same time, sputum samples were collected and processed as previously described [44], with minor modifications. Briefly, expectorates were collected directly from a patient and immediately added to freshly prepared sputum pre-lysis and preservation buffer (3 ml $1 \times$ DNA/RNA shield per 1–2 ml sputum sample, Zymo Research, USA; 200 mM Tris(2-carboxyethyl)phosphine, TCEP; 100 μ g/ml Proteinase K, Thermo Fisher Scientific, USA) and vigorously shaken by hand until the samples were homogenous and wholly lysed. Samples were briefly stored at 4 °C and then at –80 °C for long-term storage.

3.2. Antibodies and flow cytometry

A highly standardized, customized DuraClone antibody panel [45] (Beckman Coulter, USA), specially developed for immune cell profiling of lymphoid and myeloid cell subsets, was used. Whole blood (50 μ L) was labeled according to the manufacturer's instructions using seven tubes containing each a lyophilized 10-plex antibody cocktail. After staining, the sample was subjected to red blood cell lysis. A complete list of the antibodies, with fluorochromes and antibody clone numbers, is provided in Table S1. The first tube contained lineage-specific antibodies and acquisition beads to assess absolute cell counts, which were used to calculate absolute concentrations of cell subsets in the remaining tubes. The samples were analyzed using Navios Ex flow cytometers (Beckman Coulter, USA). SPHERO™ Rainbow Calibration Particles (8 peaks; BD Biosciences) were used for calibration and standardization of the instruments. The optimized median fluorescence intensity (MFI) for “target values” was determined for the 6th peak of SPHERO™ Rainbow Calibration Particles on the first cytometer, and these optimized detector voltages were used as target values of the 2nd cytometer. SPHERO™ Rainbow Calibration Particles were finally used to compare the inter-instrument standardized cytometer settings. The instruments' performance was monitored over time using peak-3 and peak-6 of

Rainbow Calibration Particles (MFI and SD values), checking the Flow-instruments setup between and over time.

The acquired sample data were analyzed using serial gating strategies in standardized predefined analysis templates in Kaluza software 2.1 (Beckman Coulter, USA). Examples of the gating strategy are shown in Fig. S5. A complete list of gated cell populations and their marker combinations can be found in Table S2. Data exported from Kaluza were processed in a custom script to calculate absolute concentrations, after which visualization and statistical analyses were performed using R software (version 4.2.1) and GraphPad Prism (version 9.4.1).

Gated cell populations were analyzed by principal component analysis (PCA) using the R package “FactorMineR”. Missing data were imputed by a PCA method using the R package “missMDA”. Hierarchical cluster analysis and K-means clustering were performed on \log_{10} -transformed data using “pheatmap” and “stats” package in R, respectively. Hierarchical clustering was performed using the complete agglomeration method with Euclidian distances. Categorical variables were compared using the χ^2 test. Correlations were calculated using Spearman's rho rank correlation analysis using the “Hmisc” R package.

3.3. Sputum sample processing and sequencing library preparation

Frozen sputum samples were thawed at room temperature. After adding 1 mg/mL lysozyme, samples were incubated for 10 min at room temperature and then for another 10 min on ice. Samples were homogenized in ZR BashingBead Lysis Tubes (Zymo Research, USA), performing 3 homogenization cycles (30 s at 6500 rpm and 2 min incubation on ice) using Precellys 24 homogenizer (Bertin Instruments, USA). Total RNA was extracted using Quick-DNA/RNA Miniprep (Zymo Research, USA). Between 0.8 – 5 μ g of total RNA was digested with 6 – 10 U of TURBO DNase (Thermo Fisher Scientific, USA) for 30 min. DNase-digested RNA was purified using the RNA Clean & Concentrator-5 kit (Zymo Research, USA), selecting RNA species larger than 200 bp. The recovered RNA was quantified using fluorometric quantitation, and the fragmentation state (DV_{200}) was evaluated using an RNA Nano kit on an Agilent Bioanalyzer 2100 machine (Agilent Technologies). All samples with a DV_{200} between 50% and 97% were further processed. Between 250 ng and 1 μ g of DNase-digested samples were depleted of rRNA species using a custom combination of riboPOOL Human:Pan-Bacteria (78:22 ratio) kits (siTOOLS Biotech, Germany). rRNA-depleted samples were used to prepare strand-specific sequencing libraries using the KAPA RNA HyperPrep Kit (Roche, Switzerland). After optimization, the fragmentation step time was reduced to 3 min to overcome the partially fragmented nature of the samples. Sequencing was performed on an Illumina NextSeq 500 machine, generating a minimum of 150 million reads per sample of either 1×75 bp or 2×75 bp reads.

3.4. Lung microbiome analysis

Low-quality bases and contaminant adapters were trimmed using Trimmomatic (v 0.35), discarding reads shorter than 35 nt (minimum length to avoid excessive human reads contamination in meta-transcriptomes). Reads were further processed using the SortMeRNA tool (v 2.1) to remove reads generated from residual rRNA transcripts. High-quality human and bacterial reads were separated *in silico* by mapping reads using the BWA aligner and MEM algorithm against the human genome assembly GRCh38.p9 retrieved from the NCBI database. Reads not mapping on the human genome were used as input for analyzing the transcriptionally active bacterial community identifying bacterial genera using the KRAKEN tool (version 2.1.2). Kraken output was processed with the Bracken tool (version 2.6.2) to obtain the final Operation taxonomic units (OUTs) tables. Taxa with less than five predicted fragments assigned were removed, and fragment counts were used to calculate each taxon's fraction in the samples. Taxa less than 0.1% in at least 6% of the samples ($n = 3$) were discarded. Normalized

fractions were used to calculate samples' beta diversity based on Generalized UniFrac (with alpha 0.5) metric using the GUniFrac() function from the GUniFrac R package and a phylogenetic tree generated using ETE Toolkit. Permutational multivariate ANOVA (PERMANOVA) and Mantel test, as implemented in the "vegan" R package, were used to evaluate relationships between respiratory bacterial composition (β -diversity) and patients' immune groups and ppFEV₁ parameter, respectively. Spearman's rho rank correlation analysis was used to compute correlations between microbial taxa's relative abundance and immune cells' abundance and fraction.

3.5. Statistics

All statistical analyses were performed using GraphPad Prism and R software and are reported together with statistical significance and error bars in figure legends or the appropriate section of materials and methods.

Ethical approval and consent to participate

The local ethics committee approved using the samples at the Capital Region of Denmark Region Hovedstaden (registration number H-19,001,151, approved 07/03/2019), and all patients gave informed consent according to the current laws.

Data sharing

Raw sequence read data supporting the results of this work are available in the EMBL-EBI European Nucleotide Archive (ENA) under Accession No. PRJEB56242.

CRedit authorship contribution statement

Elio Rossi: Conceptualization, Methodology, Formal analysis, Investigation, Data curation, Visualization, Writing – original draft, Writing – review & editing, Supervision, Funding acquisition. **Mads Lausen:** Formal analysis, Investigation, Data curation, Visualization, Writing – original draft, Writing – review & editing. **Nina Friesgaard Øbro:** Formal analysis, Investigation, Visualization, Writing – original draft, Writing – review & editing. **Antonella Colque:** Investigation, Writing – review & editing. **Bibi Uhre Nielsen:** Resources, Data curation, Supervision, Writing – review & editing. **Rikke Møller:** Resources, Data curation, Writing – review & editing. **Camilla de Gier:** Resources. **Annette Hald:** Resources. **Marianne Skov:** Resources, Data curation, Writing – review & editing. **Tacjana Pressler:** Resources, Data curation, Writing – review & editing. **Søren Molin:** Conceptualization, Writing – review & editing, Funding acquisition. **Sisse Rye Ostrowski:** Conceptualization, Resources, Writing – review & editing. **Hanne Vibeke Marquart:** Conceptualization, Methodology, Resources, Writing – review & editing. **Helle Krogh Johansen:** Conceptualization, Funding acquisition, Resources, Supervision, Writing – review & editing.

Declaration of competing interest

We declare no competing interests.

Acknowledgement

This research was funded by The Novo Nordisk Foundation Project Grants in Bioscience and Basic Biomedicine (grant n. NNF18OC0052776) and by a Challenge Grant (Ref. nr.: NNF19OC0056411) and a grant from the Danish Research Council (DFR-9039-00037A) awarded to HKJ. ER was supported by a Cariplo Foundation "Biomedical research conducted by young researchers" grant n. 2020-3581.

Supplementary materials

Supplementary material associated with this article can be found, in the online version, at [doi:10.1016/j.jcf.2024.04.015](https://doi.org/10.1016/j.jcf.2024.04.015).

References

- [1] Kerem E, Corey M, Kerem B, Rommens J, Markiewicz D, Levison H, et al. The Relation between Genotype and Phenotype in Cystic Fibrosis — Analysis of the Most Common Mutation ($\Delta F508$). *New Engl J Medicine* 1990;323:1517–22. <https://doi.org/10.1056/nejm199011293232203>.
- [2] Cohen TS, Prince A. Cystic fibrosis: a mucosal immunodeficiency syndrome. *Nat Med* 2012;18:509–19. <https://doi.org/10.1038/nm.2715>.
- [3] Giacalone VD, Dobosh BS, Gaggari A, Tirouvanziam R, Margaroli C. Immunomodulation in cystic fibrosis: why and how? *Int J Mol Sci* 2020;21:3331. <https://doi.org/10.3390/ijms21093331>.
- [4] Verhaeghe C, Delbecq K, de Leval L, Oury C, Bours V. Early inflammation in the airways of a cystic fibrosis foetus. *J Cyst Fibros* 2007;6:304–8. <https://doi.org/10.1016/j.jcf.2006.12.001>.
- [5] Butnariu LI, Țarcă E, Cojocaru E, Rusu C, Moisă Ștefana M, Constantin MML, et al. Genetic modifying factors of cystic fibrosis phenotype: a challenge for modern medicine. *J Clin Medicine* 2021;10:5821. <https://doi.org/10.3390/jcm10245821>.
- [6] Cuthbertson L, Walker AW, Oliver AE, Rogers GB, Rivett DW, Hampton TH, et al. Lung function and microbiota diversity in cystic fibrosis. *Microbiome* 2020;8:45. <https://doi.org/10.1186/s40168-020-00810-3>.
- [7] Tony-Odigie A, Wilke L, Boutin S, Dalpke AH, Yi B. Commensal bacteria in the cystic fibrosis airway microbiome reduce *P. aeruginosa* induced inflammation. *Front Cell Infect Mi* 2022;12:824101. <https://doi.org/10.3389/fcimb.2022.824101>.
- [8] Pressler T, Bohmova C, Conway S, Dumcius S, Hjelte L, Høiby N, et al. Chronic pseudomonas aeruginosa infection definition: euroCareCF working group report. *J Cyst Fibros* 2011;10:S75–8. [https://doi.org/10.1016/s1569-1993\(11\)60011-8](https://doi.org/10.1016/s1569-1993(11)60011-8).
- [9] Lara-Reyna S, Holbrook J, Jarosz-Griffiths HH, Peckham D, McDermott MF. Dysregulated signalling pathways in innate immune cells with cystic fibrosis mutations. *Cell Mol Life Sci* 2020;77:4485–503. <https://doi.org/10.1007/s00018-020-03540-9>.
- [10] Zhang Y, Ma CJ, Wang JM, Ji XJ, Wu XY, Jia ZS, et al. Tim-3 negatively regulates IL-12 expression by monocytes in HCV infection. *PLoS ONE* 2011;6:e19664. <https://doi.org/10.1371/journal.pone.0019664>.
- [11] Kumamoto Y, Hirai T, Wong PW, Kaplan DH, Iwasaki A. CD301b+ dendritic cells suppress T follicular helper cells and antibody responses to protein antigens. *Elife* 2016;5:e17979. <https://doi.org/10.7554/elife.17979>.
- [12] Aridgides DS, Mellinger DL, Gwilt LL, Hampton TH, Mould DL, Hogan DA, et al. Comparative effects of CFTR modulators on phagocytic, metabolic and inflammatory profiles of CF and non-CF macrophages. *Sci Rep* 2023;13:11995. <https://doi.org/10.1038/s41598-023-38300-9>.
- [13] Pollock J, Chalmers JD. The immunomodulatory effects of macrolide antibiotics in respiratory disease. *Pulm Pharmacol Ther* 2021;71:102095. <https://doi.org/10.1016/j.pupt.2021.102095>.
- [14] Thornton CS, Acosta N, Surette MG, Parkins MD. Exploring the cystic fibrosis lung microbiome: making the most of a sticky situation. *J Pediatric Infect Dis Soc* 2022; 11:S13–22. <https://doi.org/10.1093/jpids/piac036>.
- [15] Laval J, Ralhan A, Hartl D. Neutrophils in cystic fibrosis. *Biol Chem* 2016;397: 485–96. <https://doi.org/10.1515/hsz-2015-0271>.
- [16] Hector A, Schäfer H, Pöschel S, Fischer A, Fritzscheing B, Ralhan A, et al. Regulatory T-cell impairment in cystic fibrosis patients with chronic pseudomonas infection. *Am J Resp Crit Care* 2015;191:914–23. <https://doi.org/10.1164/rccm.201407-1381oc>.
- [17] Xu Y, Krause A, Limberis M, Worgall TS, Worgall S. Low sphingosine-1-phosphate impairs lung dendritic cells in cystic fibrosis. *Am J Resp Cell Mol* 2013;48:250–7. <https://doi.org/10.1165/rcmb.2012-0021oc>.
- [18] Tsuda Y, Takahashi H, Kobayashi M, Hanafusa T, Herndon DN, Suzuki F. Three different neutrophil subsets exhibited in mice with different susceptibilities to infection by methicillin-resistant staphylococcus aureus. *Immunity* 2004;21: 215–26. <https://doi.org/10.1016/j.immuni.2004.07.006>.
- [19] Garrison SP, Thornton JA, Häcker H, Webby R, Rehg JE, Parganas E, et al. The p53-target gene puma drives neutrophil-mediated protection against lethal bacterial sepsis. *Plos Pathog* 2010;6:e1001240. <https://doi.org/10.1371/journal.ppat.1001240>.
- [20] Sigua JA, Buelow B, Cheung DS, Buell E, Hunter D, Klancnik M, et al. CD49d-expressing neutrophils differentiate atopic from nonatopic individuals. *J Allergy Clin Immunol* 2014;133:901–4. <https://doi.org/10.1016/j.jaci.2013.09.035>.
- [21] Antunes J, Fernandes A, Borrego LM, Leiria-Pinto P, Cavaco J. Cystic fibrosis, atopy, asthma and ABPA. *Allergol Immunopath* 2010;38:278–84. <https://doi.org/10.1016/j.aller.2010.06.002>.
- [22] Long A, Kleiner A, Looney RJ. Immune dysregulation. *J Allergy Clin Immunol* 2023;151:70–80. <https://doi.org/10.1016/j.jaci.2022.11.001>.
- [23] Tiringir K, Treis A, Fucik P, Gona M, Gruber S, Renner S, et al. A Th17- and Th2-skewed cytokine profile in cystic fibrosis lungs represents a potential risk factor for pseudomonas aeruginosa infection. *Am J Resp Crit Care* 2013;187:621–9. <https://doi.org/10.1164/rccm.201206-1150oc>.
- [24] Belkaid Y, Rouse BT. Natural regulatory T cells in infectious disease. *Nat Immunol* 2005;6:353–60. <https://doi.org/10.1038/nri181>.

- [25] Rigauts C, Aizawa J, Taylor SL, Rogers GB, Govaerts M, Cos P, et al. *Rothia mucilaginosa* is an anti-inflammatory bacterium in the respiratory tract of patients with chronic lung disease. *Eur Respir J* 2022;59:2101293. <https://doi.org/10.1183/13993003.01293-2021>.
- [26] Bocchino M, Zanotta S, Capitelli L, Galati D. Dendritic cells are the intriguing players in the puzzle of idiopathic pulmonary fibrosis pathogenesis. *Front Immunol* 2021;12:664109. <https://doi.org/10.3389/fimmu.2021.664109>.
- [27] Kumamoto Y, Linehan M, Weinstein JS, Laidlaw BJ, Craft JE, Iwasaki A. CD301b+ dermal dendritic cells drive T helper 2 cell-mediated immunity. *Immunity* 2013;39:733–43. <https://doi.org/10.1016/j.immuni.2013.08.029>.
- [28] Linehan JL, Dileepan T, Kashem SW, Kaplan DH, Cleary P, Jenkins MK. Generation of Th17 cells in response to intranasal infection requires TGF- β 1 from dendritic cells and IL-6 from CD301b+ dendritic cells. *Proc National Acad Sci* 2015;112:12782–7. <https://doi.org/10.1073/pnas.1513532112>.
- [29] Lachenal F, Nkana K, Nove-Josserand R, Fabien N, Durieu I. Prevalence and clinical significance of auto-antibodies in adults with cystic fibrosis. *Europ Respir J* 2009;34:1079–85. <https://doi.org/10.1183/09031936.00006009>.
- [30] Moratto D, Gulino AV, Fontana S, Mori L, Pirovano S, Soresina A, et al. Combined decrease of defined B and T cell subsets in a group of common variable immunodeficiency patients. *Clin Immunol* 2006;121:203–14. <https://doi.org/10.1016/j.clim.2006.07.003>.
- [31] Ahn S, Cunningham-Rundles C. Role of B cells in common variable immune deficiency. *Expert Rev Clin Immunol* 2009;5:557–64. <https://doi.org/10.1586/eci.09.43>.
- [32] Frija-Masson J, Martin C, Regard L, Lothe M-N, Touqui L, Durand A, et al. Bacteria-driven peribronchial lymphoid neogenesis in bronchiectasis and cystic fibrosis. *Eur Respir J* 2017;49:1601873. <https://doi.org/10.1183/13993003.01873-2016>.
- [33] Menon M, Hussell T, Shuwa HA. Regulatory B cells in respiratory health and diseases. *Immunol Rev* 2021;299:61–73. <https://doi.org/10.1111/imr.12941>.
- [34] Warnatz K, Wehr C, Dräger R, Schmidt S, Eibel H, Schlesier M, et al. Expansion of CD19hiCD21lo/neg B cells in common variable immunodeficiency (CVID) patients with autoimmune cytopenia. *Immunobiology* 2002;206:502–13. <https://doi.org/10.1078/0171-2985-00198>.
- [35] Unger S, Seidl M, van Schouwenburg P, Rakhmanov M, Bulashevskaya A, Frede N, et al. The TH1 phenotype of follicular helper T cells indicates an IFN- γ -associated immune dysregulation in patients with CD21low common variable immunodeficiency. *J Allergy Clin Immunol* 2018;141:730–40. <https://doi.org/10.1016/j.jaci.2017.04.041>.
- [36] Segal LN, Clemente JC, Tsay J-CJ, Korolov SB, Keller BC, Wu BG, et al. Enrichment of the lung microbiome with oral taxa is associated with lung inflammation of a Th17 phenotype. *Nat Microbiol* 2016;1:16031. <https://doi.org/10.1038/nmicrobiol.2016.31>.
- [37] Garcia BJ, Loxton AG, Dolganov GM, Van TT, Davis JL, BC de Jong, et al. Sputum is a surrogate for bronchoalveolar lavage for monitoring *Mycobacterium tuberculosis* transcriptional profiles in TB patients. *Tuberculosis* 2016;100:89–94. <https://doi.org/10.1016/j.tube.2016.07.004>.
- [38] Zemanick ET, Wagner BD, Robertson CE, Stevens MJ, Szefer SJ, Accurso FJ, et al. Assessment of airway microbiota and inflammation in cystic fibrosis using multiple sampling methods. *Ann Am Thorac Soc* 2015;12:221–9. <https://doi.org/10.1513/annalsats.201407-310oc>.
- [39] Zhao CY, Hao Y, Wang Y, Varga JJ, Stecenko AA, Goldberg JB, et al. Microbiome data enhances predictive models of lung function in people with cystic fibrosis. *J Infect Dis* 2020;223:S246–56. <https://doi.org/10.1093/infdis/jiaa655>.
- [40] Ichikawa T, Hirahara K, Kokubo K, Kiuchi M, Aoki A, Morimoto Y, et al. CD103hi Treg cells constrain lung fibrosis induced by CD103lo tissue-resident pathogenic CD4 T cells. *Nat Immunol* 2019;20:1469–80. <https://doi.org/10.1038/s41590-019-0494-y>.
- [41] O'Neal WK, Gallins P, Pace RG, Dang H, Wolf WE, Jones LC, et al. Gene expression in transformed lymphocytes reveals variation in endomembrane and HLA pathways modifying cystic fibrosis pulmonary phenotypes. *Am J Hum Genet* 2015;96:318–28. <https://doi.org/10.1016/j.ajhg.2014.12.022>.
- [42] Adriaanse MPM, Vreugdenhil ACE, Groeneweg M, Brüggewirth HT, Castelijns SJAM, der Ent CK van, et al. HLA frequencies and associations in cystic fibrosis. *Tissue Antigens* 2014;83:27–31. <https://doi.org/10.1111/tan.12265>.
- [43] Nichols DP, Morgan SJ, Skalland M, Vo AT, Dalfens JMV, Singh SBP, et al. Pharmacologic improvement of CFTR function rapidly decreases sputum pathogen density but lung infections generally persist. *J Clin Invest* 2023. <https://doi.org/10.1172/jci167957>.
- [44] Rossi E, Falcone M, Molin S, Johansen HK. High-resolution in situ transcriptomics of *Pseudomonas aeruginosa* unveils genotype independent patho-phenotypes in cystic fibrosis lungs. *Nat Commun* 2018;9:3459. <https://doi.org/10.1038/s41467-018-05944-5>.
- [45] Ronit A, Berg RMG, Bay JT, Haugaard AK, Ahlström MG, Burgdorf KS, et al. Compartmental immunophenotyping in COVID-19 ARDS: a case series. *J Allergy Clin Immunol* 2021;147:81–91. <https://doi.org/10.1016/j.jaci.2020.09.009>.